ONLINE APPENDIX

Precision Medicine in Cardiac Channelopathy: Integrating Genome Editing and Induced Pluripotent Stem Cells to Decipher Variant of Unknown Significance

Priyanka Garg, PhD[a, b, c], Angelos Oikonomopoulos, PhD[a, b, c], Haodong Chen, PhD[a, b, c], Yingxin Li, PhD[a, b, c], Chi Keung Lam, PhD[a, b, c], Karim Sallam, MD[a, b, c], Marco Perez, MD[d], Robert L. Lux, PhD[e], Michael C. Sanguinetti, PhD[e, f], Joseph C. Wu, MD, PhD[a, b, c]

[a]Stanford Cardiovascular Institute, [b]Department of Medicine, Division of Cardiology, [c]Institute for Stem Cell Biology and Regenerative Medicine, [d]Center for Inherited Cardiovascular Disease, Division of Cardiovascular Medicine, Stanford University, Stanford, CA. [e]Nora Eccles Harrison Cardiovascular Research and Training Institute, [f]Division of Cardiovascular Medicine, Department of Internal Medicine, University of Utah, Salt Lake City, Utah.

SUPPLEMENTAL METHODS

Mutation analysis. SNP (rs149955375) was confirmed by TaqMan SNP Genotyping Assay (C_173430597_10; Thermo Fisher Scientific) following the manufacturer's protocol using genomic DNA isolated from either healthy control or VUS patient iPSCs.

Immunofluorescence staining. Immunofluorescence was performed using appropriate primary antibodies and AlexaFluor-conjugated secondary antibodies (Invitrogen) as described by the manufacturer's protocol. The primary antibodies used in this study were SOX2 (Biolegend, San Diego, CA), NANOG (Santa Cruz, CA), cardiac Troponin T (cTnT) (Abcam, ab10214), sarcomeric α-actinin (Abcam, ab90776), and hKv11.1 (Abcam, ab136467).

Flow cytometry. iPSC-CMs were fixed in BD Cytofix/Cytoperm (BD 554722) solution for 20 min on ice, washed with 1X BD Perm/Wash buffer, stained overnight in 4°C with rabbit anti-cardiac Troponin T antibody (1:200, Abcam # ab45932) and mouse monoclonal anti-alpha-actinin antibody (1:200 Sigma # A7811), and labeled on ice for 30 min with goat anti-mouse IgG (H+L) secondary antibody, Alexa Fluor® 647 conjugate (1:250, Thermo Fisher Scientific # A21235), and goat anti-rabbit IgG (H+L) secondary antibody, Alexa Fluor® 488 conjugate (1:250, Thermo Fisher Scientific # A11034). Data were acquired using BD FACS Aria II in the FACS Core at the Stanford Institute for Stem Cell Biology and Regenerative Medicine, and analyzed using FlowJo software (FlowJo, LLC).

Immunoblot analysis. iPSC-CMs were washed with ice-cold PBS and incubated with RIPA assay buffer containing (Sigma) and HaltTM protease and phosphatase inhibitor cocktail

(Thermo Scientific). The insoluble debris was removed by centrifugation (14,000 rpm, 5 min, and 4°C) and protein concentration was determined by Pierce BCA Protein assay kit (Thermo Scientific). Equal amounts of protein lysates (12 µg) were loaded in 4-10% mini-Protean TGX Stain-free polyacrylamide gels (BIO-RAD) and transferred to a nitrocellulose membrane. The membrane was blocked with 1X TBS-T containing 0.1% Tween-20 and 5% non-fat dry milk. Primary antibodies against KCNH2 (Cell Signaling) and GAPDH (Thermo Scientific) were incubated with the membranes overnight at 4°C under constant shaking. Appropriate secondary antibodies (Sigma) were incubated with the membranes for 2 hr at ambient temperature. Membranes were washed with 1X TBS-T containing 0.1% Tween-20. Enhanced chemiluminescence (ECL) was applied for the detection of horseradish peroxidase (HRP) activity from protein probes.

CRISPR/Cas9 and ssDNA Transfections. iPSCs were enzymatically dissociated with Accutase (Sigma) and plated on Matrigel-coated dishes at 1:4 ratio in E8 medium supplemented with 10 µmol/L Y-27632 (Selleck Chemicals). Twenty-four hours later, healthy control or VUS iPSCs were transfected with the combination of CRISPR/Cas9 plasmid vector containing the designed *KCNH2* gRNA (1-2 µg) and the respective ssDNA (4 µg) for the editing and the correction of the *KCNH2*$^{2948C>T}$ and *KCNH2*$^{2948T>C}$ mutations, using Lipofectamine 3000 according to the instructions of the manufacturer. Forty eight hours following transfection, GFP-expressing iPSCs were collected via fluorescence-activated cell sorting (FACSAria II; BD Biosciences) and were cultured in Matrigel pre-coated 24-well plates in E8 medium supplemented with 10 µmol/L Y-27632 at single-cell density (200 cells/cm^2). Seven to ten days later, single-cell derived iPSC colonies were manually picked for sub-culturing and genomic DNA-screening.

Screening of genome-edited iPSC clones. Genomic DNA was isolated from iPSCs using the Phire Animal Tissue Direct PCR kit (Thermo Scientific) according to the instructions of the manufacturer. The following primers were used for the screening of the genome-edited and corrected *KCNH2* alleles (KCNH2_For: TGTTTCCCACAGACACGGAG and KCNH2_Rev: TCTACCAGACAACACCGCCA). Genomic DNA was used for PCR analysis using the high fidelity PrimeSTAR GXL DNA Polymerase (Clontech, Takara) according to the instructions of the manufacturer. PCR products were analyzed by DNA sequencing and successfully genome-edited iPSCs were further expanded for subsequent experimentation as indicated in the manuscript.

Electrophysiological recordings of iPSC-CMs. Whole-cell patch clamp recordings from iPSC-CMs were performed using an EPC-10 patch clamp amplifier (HEKA, Lambrecht, Germany) and a RC-26C recording chamber (Warner Instruments, Hamden, CT) mounted onto the stage of an inverted microscope (Nikon, Tokyo, Japan). Contracting monolayer of iPSC-CMs was mechanically removed from plate, enzymatically dispersed into single cells, and attached to Matrigel-coated glass coverslips (Warner Instruments). Current-clamp technique was utilized to record action potentials from iPSC-CMs at 36-37°C. Voltage-clamp technique was used to record I_{Kr} from iPSC-CMs at room temperature. Data were digitized at 1.0 kHz and acquired using PatchMaster software (HEKA, Germany) and analyzed using FitMaster (HEKA, Germany), Igor Pro (Wave Metrics), and Origin 2016 (OriginLab, Northampton, MA). Temperature was kept constant by a TC-324B heating system (Warner, USA) at 36-37°C. To obtain action potentials from iPSC-CMs, current clamp recordings were conducted in normal Tyrode's solution containing 150 mM NaCl, 5.4 mM KCl, 1 mM $MgCl_2$, 15 mM glucose, 1.8

mM $CaCl_2$, 15 mM HEPES, and 1 mM sodium pyruvate (pH 7.4 with NaOH at 25°C). The pipette solution contained 120 mM KCl, 1 mM $MgCl_2$, 10 mM HEPES, 3 mM Mg-ATP, and 10 mM EGTA (pH 7.2 with KOH at 25°C). To record I_{Kr}, defined as the E-4031 (2 μM) sensitive current subtracted by the current recorded before and after E-4031 application from iPSC-CMs, voltage clamp recordings were conducted at room temperature. External and internal solution compositions were essentially the same as those used for current clamp recordings, except that 10 μM chromanol and 400 nM nisoldipine were added to the external solution to block the slow component of the delayed rectifier potassium current (I_{Ks}) and the L-type calcium current (I_{CaL}), respectively. I_{Kr} was elicited by 2.5-s depolarizing steps from a holding potential of -50 mV to potentials ranging from -50 to +40 mV in 10 mV increments. This was followed by a 4-s repolarization phase to -40 mV to elicit the tail current. All data are expressed as mean ± S.E.M. Student's t-test was used to evaluate statistical significance.

Two-electrode voltage clamp of *Xenopus* oocytes. HERG1 (*KCNH2*, isoform 1a, National Center for Biological Technology Information Reference Sequence: NM_000238.2) was cloned into the pSP64 oocyte expression vector. T983I mutation in wild-type (WT) hERG cDNA was made using the QuikChange site-directed mutagenesis kit (Agilent Technologies, Santa Clara, CA) and was verified by DNA sequence analyses. cRNAs were prepared using the mMessage mMachine SP6 kit (Ambion, Austin, TX) and quantified using RiboGreen assay (Life Technologies). Procedures for harvesting oocytes from *Xenopus laevis* were described elsewhere (1) and were approved by the University of Utah Institutional Animal Care and Use Committee. The isolation, culture, and injection of oocytes with cRNA were performed as described previously (2). Injected oocytes were incubated for 1–5 days at 18°C in Barth's saline solution

before use in voltage clamp experiments. Currents were recorded from oocytes with the use of a standard two-microelectrode voltage clamp technique (2) and agarose-cushion micro- electrodes (3). A GeneClamp 500 amplifier, Digidata 1322A data acquisition system, and pCLAMP 9.0 software (Molecular Devices, Inc., Sunnyvale, CA) were used to produce command voltages and to record current and voltage signals. Oocytes were bathed in KCM211 solution at room temperature (22 – 24°C). To record ionic currents, oocytes were voltage clamped to a holding potential of -80 mV. After a brief (100 ms) prepulse to -70 mV, step currents were elicited with 4-s pulses from -70 to +40 mV in 10-mV increments. Tail currents were measured at -70 mV by a 3.5 s long pulse. Barth's solution contained 88 mM NaCl, 2 mM KCl, 0.41 mM $CaCl_2$, 0.33 mM $Ca(NO_3)_2$, 1 mM $MgSO_4$, 2.4 mM $NaHCO_3$, 10 mM HEPES, 1 mM pyruvate, and 50 mg/l gentamycin; pH was adjusted to 7.4 with NaOH. KCM211 solution contained 98 mM NaCl, 2 mM KCl, 1 mM $CaCl_2$, 1 mM $MgCl_2$, and 5 mM HEPES; pH was adjusted to 7.6 with NaOH.

Microelectrode array recordings. iPSC-CMs were dissociated enzymatically using Accutase (Sigma). The resulting cell suspension was transferred to a 15 ml conical tube and centrifuged at 1,000 rpm for 3 min. The supernatant was aspirated carefully without disturbing the cell pellet that was diluted with plating medium (RPMI-1640 Medium (1X, Gibco), B-27 Supplement (50X, Gibco), FBS (10%)) to 4,000,000-plated iPSC-CMs/ml. An 8 µl droplet of iPSC-CM suspension was placed over the recording electrode area of each well of the Matrigel-coated 48-well MEA plate and incubated at 37°C, 5% CO_2 for 1 hr. 200 µl of maintenance medium (RPMI-1640 Medium (1X, Gibco), B-27 Supplement (50X, Gibco)) was added to each well of the MEA plate (Axion BioSystems, USA) followed by gradually adding the remaining volume to reach the plate recommended media volume. On day 2 post-plating, the plating medium was replaced with

maintenance medium. MEA recordings were performed 10 days after plating. Electrical activity of iPSC-CMs was recorded using the Maestro recording instrument (Axion BioSystems, USA) at 37°C using the standard cardiac settings (Axion Biosystems Maestro Axis software). The field potential duration (FPD) defined as the interval between a positive or negative spike and a subsequent positive deflection was analyzed with Axion Biosystems software. Fridericia's formula was used to standardize the beat rate-associated dispersed FPD: FPDc = Fridericia's Correction = FPD/(Beat Period)^0.3333.

Ca^{2+} imaging. Dissociated iPSC-CMs were seeded on a glass cover-slip for 5-7 days after which they were loaded with the cell-permeable calcium sensitive dye fura-2 AM (2 µmol/L) for 20 min. This is followed by a 15 min washing in 1.8 mmol/L Ca^{2+}-Tyrode buffer with 135 mmol/L NaCl, 5.4 mmol/L KCl, 1 mmol/L $MgCl_2$, 5 mmol/L glucose, and 10 mmol/L HEPES (pH 7.4) to allow deesterification. Coverslips were mounted on the stage of an inverted epifluorescence microscope (Nikon Eclipse Ti-S). iPSC-CMs were field stimulated at 0.5 Hz with pulse duration of 10 ms. Fura-2 AM loaded cells were excited at both 340 and 380 nm and the emission fluorescence signal was collected at 510 nm. Changes in fluorescence signal were measured by the NIS Elements AR software, which permits recording of multiple cells in one view. Intracellular calcium changes were expressed as changes in ratio R=F340/F380 and the calcium transient waves were analyzed using the Greensmith's method (4).

Drug solutions. All drugs used in this study including E4031, nisoldipine, chromanol 293B, dofetilide, ibutilide and azimilide were purchased from Sigma-Aldrich (St. Louis, MO). ICA-105574 was purchased from AKos GmBH (Steinen, Germany). All compounds were dissolved

in DMSO and prepared as a 10 mM stock in a glass vial stored at -20^{o}C. Compounds were thawed at room temperature and all drug solutions were prepared by dilution of the stock solution with bath external solution immediately before use for each experiment.

Statistical analysis. Statistical significance was determined by unpaired Student's t-test (two-tail). * indicates $p<0.05$ and was considered statistically significant, ** indicates $p<0.01$, *** indicates $p<0.001$ when compared to control iPSC-CMs. One-way ANOVA followed by Tukey's post-hoc tests were used when comparing genome-edited iPSC lines.

SUPPLEMENTAL REFERENCES

1. Garg V, Stary-Weinzinger A, Sanguinetti MC. ICA-105574 interacts with a common binding site to elicit opposite effects on inactivation gating of EAG and ERG potassium channels. Mol Pharmacol 2013;83:805-13.
2. Stuhmer W. Electrophysiological recording from Xenopus oocytes. Methods Enzymol 1992;207:319-39.
3. Schreibmayer W, Lester HA, Dascal N. Voltage clamping of Xenopus laevis oocytes utilizing agarose-cushion electrodes. Pflugers Arch 1994;426:453-8.
4. Greensmith DJ. Ca analysis: an Excel based program for the analysis of intracellular calcium transients including multiple, simultaneous regression analysis. Comput Methods Programs Biomed 2014;113:241-50.
5. Burridge PW, Matsa E, Shukla P et al. Chemically defined generation of human cardiomyocytes. Nat Methods 2014;11:855-60.

ONLINE FIGURE LEGENDS

Online Figure 1. (A) Representative immunofluorescence images showing staining of cardiac markers cTnT (red) and α-Actinin (green) in single iPSC-CMs derived from control, VUS, VUS^{hom}, and VUS^{corr} iPSC-CMs. DAPI indicates the nuclear staining (blue). Scale bar = 10 μM. **(B)** Cardiac differentiation efficiency was calculated by the percentage of $TNNT2^{+}/ACTN^{+}$ cells using flow cytometry. All differentiated iPSC-CMs showed robust expression of cardiac markers with no significant differences among the four iPSC lines.

Online Figure 2. Two-electrode voltage-clamp recordings of overexpressed I_{Kr} in *Xenopus* oocytes. (A) Representative current traces recorded from oocytes injected with hERG WT (control, left) or hERG T983I (VUS, right) cRNA (23 nL, 1:3 dilution, oocytes incubated for 2 days after injection). The voltage step protocol is shown on the top. **(B)** Average current–voltage (*I–V*) relationships for I_{Kr} from hERG WT (blue, n = 14) and hERG T983I (grey, n = 14). **(C)** Normalized activation curve comparing hERG WT (blue) and hERG T983I (grey). Half-maximal activation voltage ($V_{1/2}$) was −27 ± 1.4 mV (n = 14) for WT and −32.5 ± 0.5 mV (n = 14) for mutant channels. * $p<0.05$ being considered statistically significant.

Online Figure 3. Analysis of the surface expression of KCNH2 protein in iPSC-CMs. (A) Representative Western blot analysis of KCNH2 protein expression in healthy control and patient-derived VUS iPSC-CMS. Core- and complex-glycosylated hERG (135 and 155 kDa, respectively) are indicated. TNNT2 (cardiac troponin T) and GAPDH (Glyceraldehyde 3-phosphate dehydrogenase) were used as internal controls. **(B)** Densitometric quantification of the mature (155 kDa) and immature (135 kDa) bands (normalized to TNNT2). **(C)** Average KCNH2

trafficking efficiency in control and VUS iPSC-CMs calculated from densitometric analysis of Western blot experiments. Trafficking efficiency is calculated as a ratio of 155 kDa band intensity to total KCNH2 band intensity. Values are represented as mean ± S.E.M., n = 4. *p<0.05.

Online Figure 4. Phenotypic characterization of classical pathogenic LQT2-A561V iPSC-CMs. (A) Representative AP recordings from LQT2-A561V iPSC-CMs showing V-like and A-like morphologies (n = 39). **(B)** Representative atrial AP recording showing arrhythmogenic activity manifested as EADs.

Online Figure 5. Patient-specific VUS iPSC-CMs displayed enhanced susceptibility to azimilide- and ibutilide-induced proarrhythmia. (A) Representative AP recordings from control (top) and VUS (bottom) at baseline (left) and after application of 5 nM ibutilide (right). **(B)** Representative AP recordings from control (top) and VUS (bottom) at baseline (left) and after application of 1 μM azimilide (right). **(C)** Summary of % increase in APD_{90} by ibutilide and azimilide for control (blue, n = 3) and VUS (grey, n = 3) iPSC-CMs. ***p<0.001. Error bars show S.E.M.

Online Figure 6. Design of CRISPR/Cas9-mediated gene editing of healthy control and VUS patient iPSC lines. (A) Representation of KCNH2 genomic locus and *KCNH2*$^{2948C>T}$ point mutation. Schematic illustration of CRISPR/Cas9-mediated gene editing of **(B)** healthy control iPSC line for the introduction of *KCNH2*$^{2948C>T}$ point mutation and **(C)** correction of the VUS patient iPSC line. Double-stranded DNA sequences represent the WT and the mutated sequences

of the healthy control and VUS patient iPSC lines, respectively. Single stranded DNA sequences (SSN) represent the oligos used for the gene editing in each case. In green letters, is depicted the gRNA oligos used for the gene editing in each case.

Online Figure 7. CRISPR/Cas9-mediated gene editing to create VUS^{hom} isogenic line and VUS^{corr} isogenic line. Confirmation by Sanger sequencing of **(A)** introduction of the *KCNH2*$^{2948C>T}$ mutation in the healthy control iPSC line and **(B)** correction of the respective mutation in the VUS patient iPSC line.

Online Figure 8. VUS^{corr} iPSC-CMs exhibited normal calcium kinetics compared to patient-specific VUS iPSCs-CMs. (A) Representative calcium transients from VUS iPSC-CMs (left) and VUS^{corr} iPSC-CMs (right) obtained from Fura-2 guided live-cell imaging. Significant arrhythmia was observed in the VUS patient line. **(B)** VUS^{corr} iPSC-CMs showed normal diastolic calcium level, while transient amplitude **(C)** was unchanged. The VUS^{corr} iPSC-CMs also displayed normal cytosolic calcium decay as indicated by faster rate constant **(D)** and shorter decay tau **(E)** compared to VUS iPSCs-CMs ***p<0.001.

ONLINE TABLE

Online Table 1. Summary of AP properties from iPSC-CMs. AP properties of spontaneously beating control, VUS, VUS^{hom}, and VUS^{corr} iPSC-CMs. MDP, maximum diastolic potential; dv/dt_{max}, maximum rise of the AP upstroke; APA, AP amplitude; APD, AP duration at different levels of repolarization (i.e., 90 or 50%); overshoot and BPM, beats per minute. To determine the type of cardiomyocyte analyzed, subtypes were specified using the following characteristics: V-

like, a negative maximum diastolic membrane potential (< -50 mV), a rapid AP upstroke, a long plateau phase, APA > 90 mV, and APD_{90}/APD_{50} ratio < 1.4. A-like, absence of a prominent plateau phase, a negative diastolic membrane potential (< -50 mV), and APD_{90}/APD_{50} ratio > 1.7. Nodal-like, a more positive MDP, a slower AP upstroke, a prominent phase 4 depolarization, and APD_{90}/APD_{50} ratio in between 1.4 - 1.7 (5). Mean values ± S.E.M. are shown. Comparison of iPSC lines was performed with one-way ANOVA with $p<0.05$ considered statistically significant.

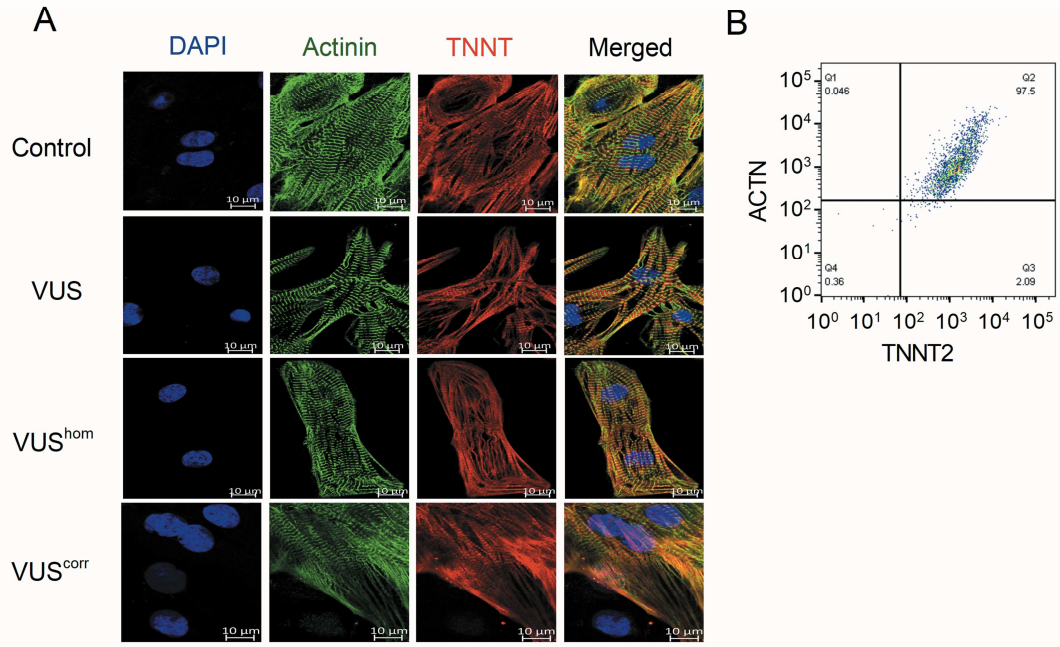

Online Figure 1

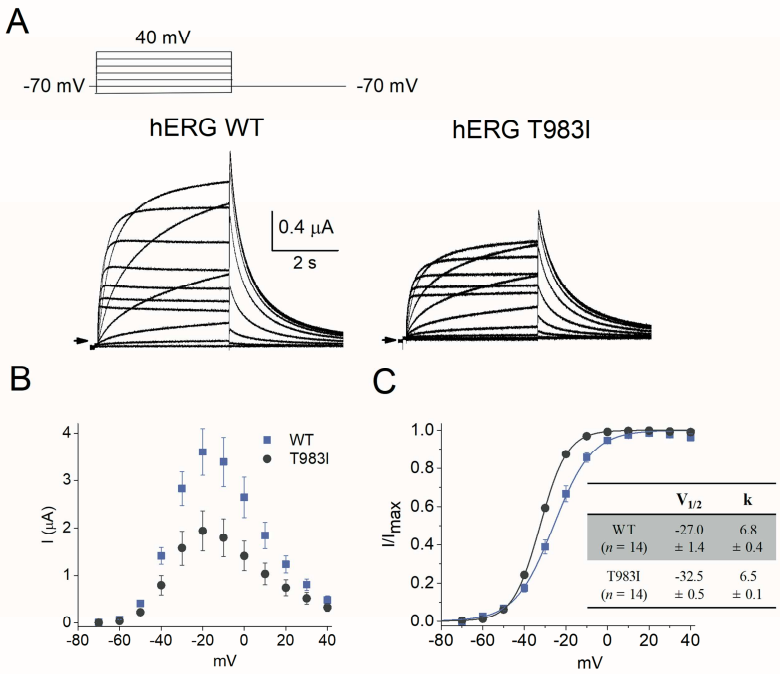

Online Figure 2

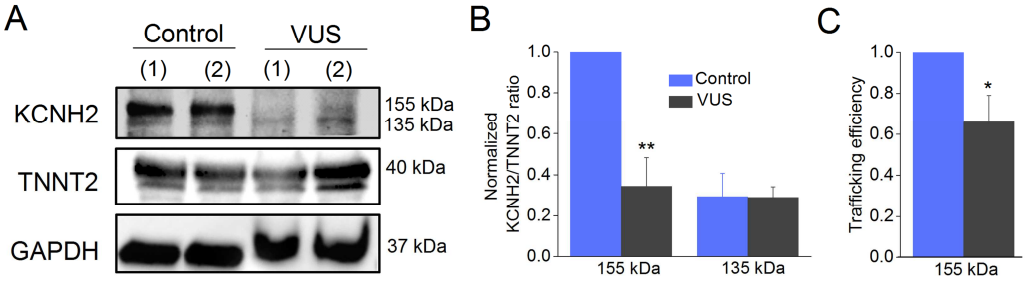

Online Figure 3

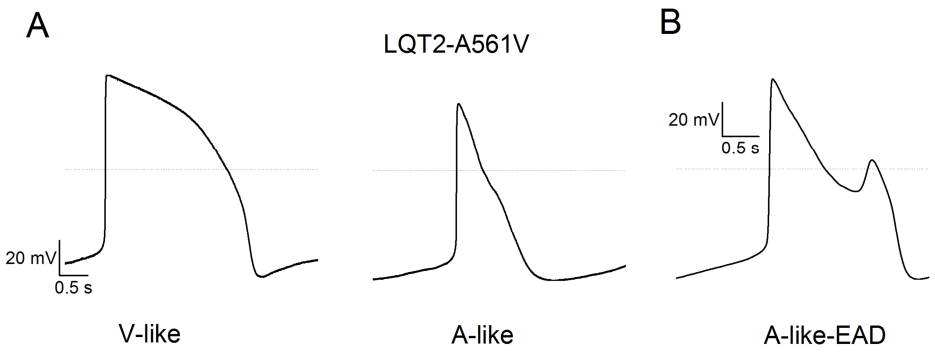

Online Figure 4

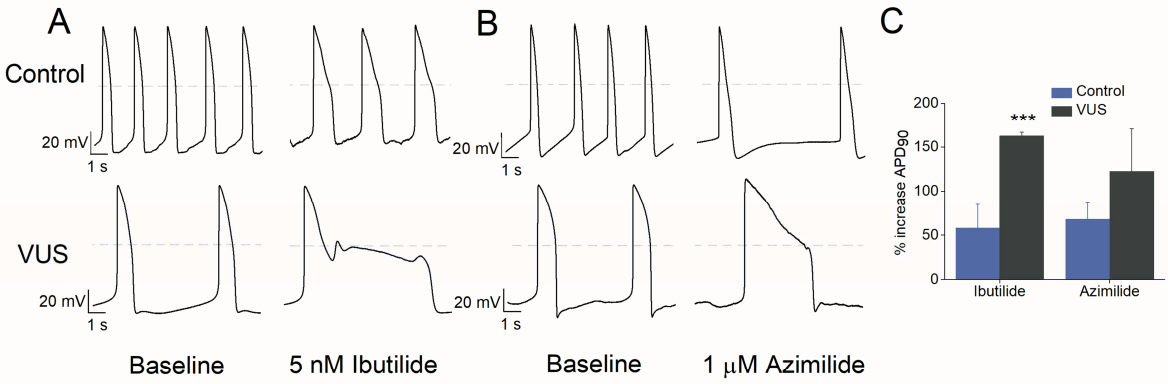

Online Figure 5

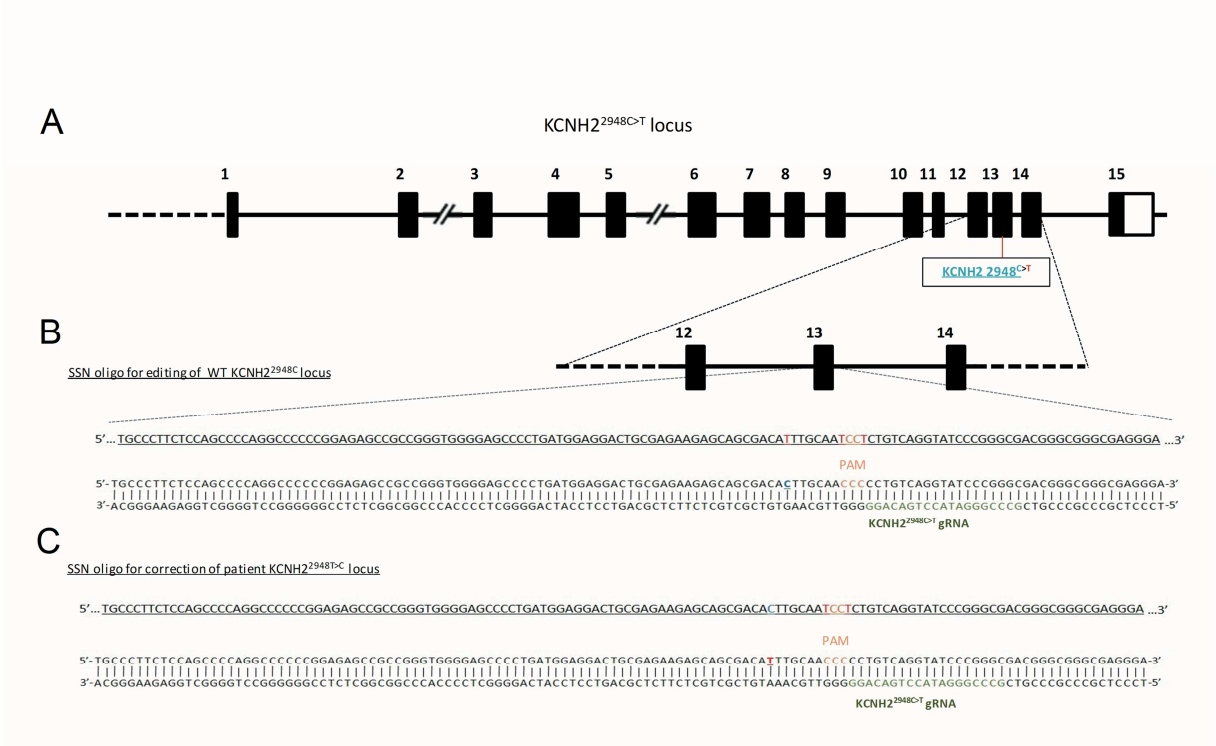

Online Figure 6

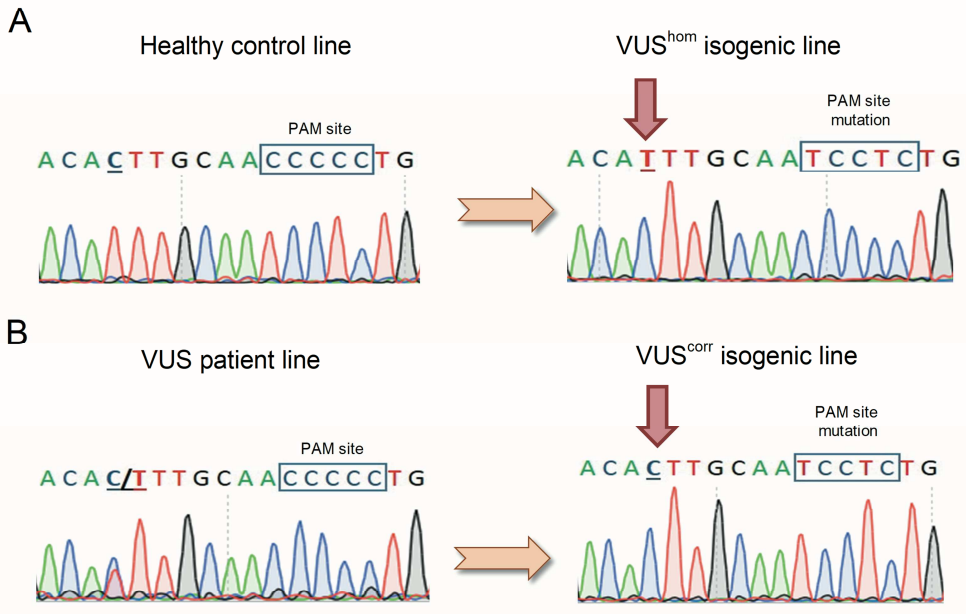

Online Figure 7

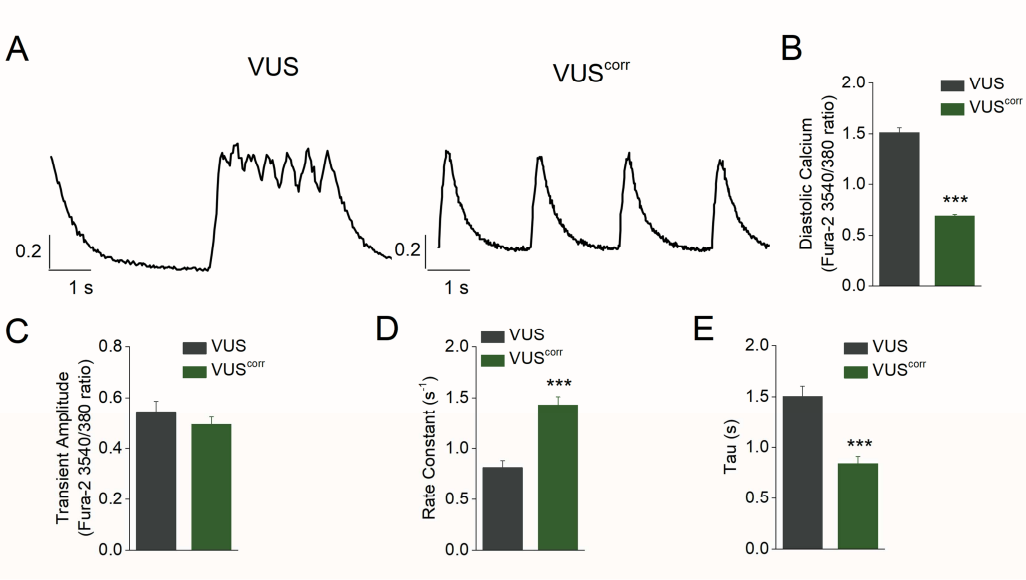

Online Figure 8

	MDP (mV)	dv/dt_{max} (V/s)	APA (mV)	APD_{90} (ms)	APD_{50} (ms)	Overshoot (mV)	BPM
Control							
V-like (*n* = 37)	-62.09 ± 0.98	21.75 ± 1.56	111.26 ± 0.99	367.17 ± 19.62	308.33 ± 17.09	48.78 ± 0.88	44.55 ± 3.89
A-like (*n* = 12)	-60.93 ± 3.53	16.12 ± 3.10	103.30 ± 3.16	288.73 ± 27.73	174.78 ± 20.46	41.32 ± 2.03	47.52 ± 6.88
VUS							
V-like (*n* = 95)	-64.46 ± 0.55	19.44 ± 0.90	110.31 ± 1.64	793.69 ± 44.13	715.81 ± 42.40	45.85 ± 1.48	38.20 ± 2.62
A-like (*n* = 24)	-61.58 ± 2.23	21.26 ± 2.31	104.91 ± 3.70	524.13 ± 47.90	389.33 ± 37.80	43.33 ± 2.16	40.21 ± 2.02
VUS^{hom}							
V-like (*n* = 19)	-59.98 ± 1.16	12.62 ± 1.03	103.80 ± 2.01	1207.91 ± 198.30	980.29 ± 167.78	43.82 ± 1.67	36.37 ± 4.08
A-like (*n* = 10)	-56.98 ± 2.89	15.49 ± 0.73	94.69 ± 3.01	605.28 ± 72.24	390.01 ± 42.82	37.71 ± 2.17	53.19 ± 5.97
VUS^{corr}							
V-like (*n* = 30)	-61.75 ± 0.15	15.16 ± 0.14	108.04 ± 0.20	452.62 ± 3.65	401.81 ± 3.55	46.91 ± 0.17	47.71 ± 0.54
A-like (*n* = 11)	-59.72 ± 1.43	14.60 ± 0.40	100.40 ± 4.60	332.19 ± 61.08	232.41 ± 40.6	41.56 ± 3.80	49.19 ± 7.04

Online Table 1. Summary of AP properties from iPSC-CMs